Z. Phys. C – Particles and Fields 35, 275–282 (1987)

Zeitschrift für Physik C Particles and Fields

Coherent production of ρ^- mesons in charged current antineutrino-neon interactions in BEBC

BEBC WA 59 Collaboration

P. Marage[3,a], M. Aderholz[9], P. Allport[10,b], N. Armenise[1], J.P. Baton[12], M. Berggren[13], D. Bertrand[3,c], V. Brisson[6], F.W. Bullock[14], W. Burkot[8], M. Calicchio[1], E.F. Clayton[7], T. Coghen[8], A.M. Cooper-Sarkar[11], O. Erriquez[1], P.J. Fitch[14], J. Guy[11], F. Hamisi[7], P.O. Hulth[13], G.T. Jones[2], P. Kasper[12], U.F. Katz[9], H. Klein[4], E. Matsinos[5], R.P. Middleton[2,b,d], D.B. Miller[7], M.M. Mobayyen[7], D.R.O. Morrison[4], M. Neveu[12], S.W. O'Neale[2], M.A. Parker[4], P. Petiau[6], J. Sacton[3], R.A. Sansum[14,b,d], N. Schmitz[9], E. Simopoulou[5], C. Vallée[6], K. Varvell[10,e], A. Vayaki[5], W. Venus[11], H. Wachsmuth[4], J. Wells[10,f], W. Wittek[9]

[1] Dipartimento di Fisica dell'Università e Sezione INFN, I-70126 Bari, Italy
[2] University of Birmingham, Birmingham, B15 2TT, UK
[3] Inter-University Institute for High Energies, ULB-VUB, B-1050 Brussels, Belgium
[4] CERN, CH-1211 Geneva 23, Switzerland
[5] Nuclear Research Centre Demokritos, GR Athens, Greece
[6] LPNHE, Ecole Polytechnique, F-91128 Palaiseau, France
[7] Imperial College of Science and Technology, London, SW7 2AZ, UK
[8] Institute of Nuclear Physics, PL-30055 Cracow, Poland
[9] Max-Planck-Institut für Physik und Astrophysik, D-8000 München 40, Federal Republic of Germany
[10] Department of Nuclear Physics, Oxford, OX1 3RH, UK
[11] Rutherford Appleton Laboratory, Chilton, Didcot, OX11 0QX, UK
[12] DPhPE, Centre d'Etudes Nucléaires, Saclay, F-91191 Gif-sur-Yvette, France
[13] Institute of Physics, University of Stockholm, S-11346 Stockholm
[14] Department of Physics and Astronomy, University College London, London WC1E 6BT, UK

Received 26 January 1987

Abstract. Coherent production of ρ^- mesons in charged current antineutrino interactions on neon nuclei is studied in the BEBC bubble chamber exposed to the CERN SPS wide band beam. The cross section is measured to be $(95 \pm 25) \cdot 10^{-40}$ cm^2 per neon nucleus, averaged over the beam energy spectrum. The distributions of kinematical variables and the absolute value of the cross section are in agreement with theoretical predictions based on the CVC hypothesis and the vector meson dominance model.

1 Introduction

The observation of coherent charged current interactions of antineutrinos on neon nuclei has been reported in a previous publication [1]. In a second publication [2], we studied the dominant contribution to that signal, the production of a single pion,

$$\bar{\nu}_\mu + \mathrm{Ne} \to \mu^+ + \pi^- + \mathrm{Ne}, \tag{1a}$$

and compared the data in this channel to theoretical predictions based on the PCAC hypothesis and the meson dominance model. In the present paper, we study another exclusive channel, the coherent production of ρ^- mesons:

$$\bar{\nu}_\mu + \mathrm{Ne} \to \mu^+ + \rho^- + \mathrm{Ne}. \tag{1b}$$

Preliminary results of this analysis have been presented elsewhere [3].

[a] Chercheur sur ARC no. 65/84–89, Belgium
[b] Now at Rutherford Appleton Laboratory
[c] Chercheur qualifié FNRS, Belgium
[d] Supported by an SERC Research Studentship, UK
[e] Now at University of Birmingham
[f] Now at University College London

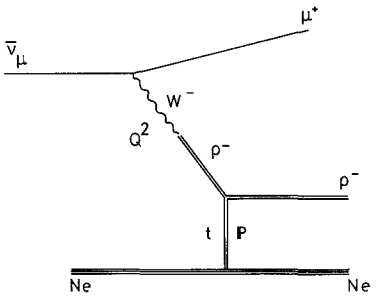

Fig. 1. Coherent diffractive production of a ρ^- meson by $\bar{\nu}_\mu$ charged current interaction on a neon nucleus

The data come from an exposure of the bubble chamber BEBC to the antineutrino wide band beam at the CERN SPS. The chamber was filled with a 75 mole% Ne/H_2 mixture in which the radiation length is 42 cm. A total of 16497 charged current antineutrino interactions with positive muons of momentum greater than 5 GeV were selected with the external muon identifier (EMI).

The discussion in this paper is based on the observation of 40 events of the type $(\mu^+\pi^-\pi^0)$ with a fully reconstructed π^0 meson and showing no evidence for nuclear breakup, with $|t|<0.1$ GeV^2, where t is the square of the 4-momentum transfer to the nucleus. The background is estimated to be (7 ± 4) events. We interpret this signal as due to coherent diffractive production of ρ^- mesons on neon nuclei (see Fig. 1).

Other experiments have searched for vector meson production in coherent (anti)neutrino interactions on nuclei: three candidates were reported by an experiment in the CERN PS antineutrino beam [4], 17 events (of which 7 were estimated to be background) were observed in an experiment in the CERN SPS neutrino beam [5], and, recently, 11 candidates were reported by an experiment at the FNAL Quadrupole Triplet Beam [6]. A signal for the diffractive production of charged ρ mesons by (anti)neutrino interactions on hydrogen or on neon has been reported by bubble chamber experiments [7–9]. The diffractive production, on hydrogen and on nuclei, of several vector mesons, and in particular of ρ^0 mesons, has been extensively studied in photo-, electro- and muoproduction [10–16].

2 The signal for coherent ρ^- production

For this analysis, the charged current events with two charged secondaries were rescanned for the possible presence of additional gammas, in order to obtain a clean sample of events in which one π^0 is produced, and to reconstruct efficiently π^0 mesons coming from ρ^- decays:

$$\rho^- \to \pi^- + \pi^0. \tag{2}$$

Figure 2a shows the (γ,γ) mass distribution for the 246 $\mu^+\pi^-\gamma\gamma$ events; this distribution peaks at the π^0 mass. Figure 3 shows the distribution of the fit probability obtained for these events when the gamma pair is constrained to come from the decay of a single π^0 meson and the fit probability P exceeds 1%; it indicates that the measurement errors are well evaluated, and that the π^0 reconstruction is reliable.

Reference 1 presents the method used for extracting the coherent signal. It is based on the fact that in coherent interactions the nucleus recoils as a whole, without breakup, giving events without stub (a stub is defined as a visible nuclear fragment or a proton of momentum less than 300 MeV). Fig. 4 shows the experimental distributions of $|t|$ for the events with a μ^+, a negatively charged hadron and a fitted π^0; $|t|$ is computed as

$$|t| = [\sum_i (E_i - p_i'')]^2 + |\sum_i \mathbf{p}_i^T|^2, \tag{3}$$

where E_i, p_i'' and $\mathbf{p}_i^T$ are the energy, the longitudinal momentum and the transverse momentum of particle

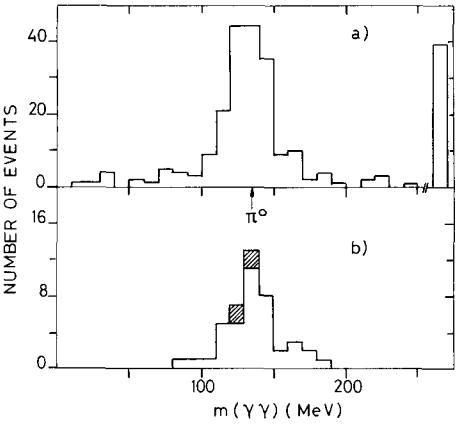

Fig. 2a, b. Distribution of the (γ,γ) mass **a** for all $(\mu^+\pi^-\gamma\gamma)$ events (246 events); **b** for the $(\mu^+\pi^-\pi^0)$ events with $|t|<0.1$ GeV^2 (44 events; the 4 events with stubs are shown hatched)

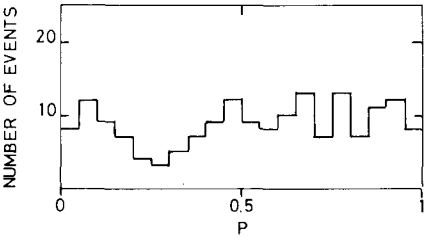

Fig. 3. Distribution of π^0 fit probability P for the $(\mu^+\pi^-\gamma\gamma)$ events, where the γ pair is constrained to come from the decay of a single π^0 meson with a probability $P>1\%$

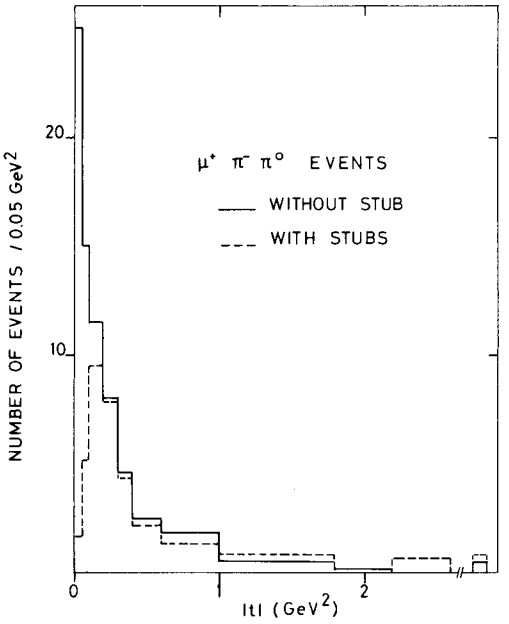

Fig. 4. Distribution of the square of the 4-momentum transfer $|t|$ for 123 ($\mu^+\pi^-\pi^0$) events without stub (full histogram) and for 53 events with stubs (dashed histogram), the latter normalised to the former in the region $|t|>0.1$ GeV^2

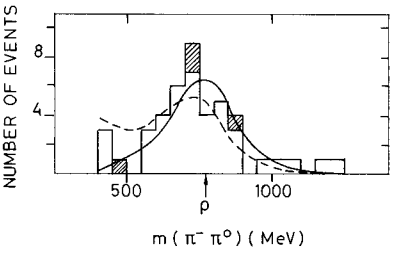

Fig. 5. Distribution of the (π^-, π^0) mass for the $(\mu^+\pi^-\pi^0)$ events with $|t|<0.1$ GeV^2 (44 events; the 4 events with stubs are shown hatched). The solid curve is the prediction of the model (4) to (12), including the effects of experimental resolution; the dashed curve includes in addition a mass skewing factor $(m_\rho/m_{\pi\pi})^n$, with $n=3$

i with respect to the neutrino direction, the sum extending over the observed final-state particles. In the case of coherent interactions, t is the square of the 4-momentum transfer to the nucleus; the peak of 40 events without stub observed at $|t|<0.1$ GeV^2 thus indicates coherent interactions. The background under this peak coming from incoherent interactions is obtained from the $|t|$-distribution of events with stubs, normalised to that of events without stub in the region $|t|>0.1$ GeV^2 (dashed histogram). The background thus estimated amounts to (7 ± 4) events, and the coherent signal is (33 ± 7) events.

The (γ,γ) mass plot for all events with $|t|<0.1$ GeV^2 is presented in Fig. 2b, the events containing stubs being shown hatched. The (π^-, π^0) mass distribution for the events with $|t|<0.1$ GeV^2 shows a clear ρ^- signal (Fig. 5)*, which appears to be free of non-resonant background.

We therefore interpret the peak in Fig. 4 at $|t|<0.1$ GeV^2 as due to coherent diffractive scattering on the neon nucleus of a ρ meson, coupled to the W boson, as indicated in Fig. 1. In coherent interactions, the virtual particle exchanged with the nucleus must neither carry charge (which would single out a nucleon) nor isospin (leading to effects of opposite sign on neutrons and protons); in addition, the exchange of ω-like objects is suppressed in the forward, low $|t|$ region. Coherent processes are thus essentially diffractive [19].

* The diffractive production of ρ^0 mesons by real or virtual photons [10–16] shows a skewing of the ρ mass shape. This is attributed to an interference of the ρ amplitude with the non-resonant dipion production [17] and is often parametrized in the form $(m_\rho/m_{\pi\pi})^n$ [18]. The solid curve in Fig. 5 represents the Breit-Wigner distribution and the kinematic $t_{\min}$ effect ($n=0$); the dashed curve corresponds to an additional skewing factor with $n=3$ [14]. The total and differential distributions discussed hereafter are insensitive to this choice; they are given for $n=0$

3 Theoretical predictions

The coherent diffractive ρ^- production cross section, based on the vector meson dominance (VMD) model as represented in Fig. 1, is [20]:

$$\frac{d^3\sigma}{dQ^2\,d\nu\,dt}=\frac{G^2}{2\pi^2}\frac{1}{\gamma_\rho^2}\left(\frac{m_\rho^2}{Q^2+m_\rho^2}\right)^2 Q^2\,\frac{\nu}{E_\nu^2}\,\frac{1}{1-\varepsilon}\cdot(1+\varepsilon R)\,\frac{d\sigma^T(\rho^-\,\mathrm{Ne}\to\rho^-\,\mathrm{Ne})}{dt} \tag{4}$$

where $G=1.166\,10^{-5}$ GeV^{-2} is the weak coupling constant; $\sqrt{2}m_\rho^2/\gamma_\rho$ is the coupling constant of the ρ^- meson to the intermediate vector boson, with $\gamma_\rho^2/4\pi\simeq2.4$ [26]; $m_\rho=0.770$ GeV is the ρ meson mass; Q^2 is the square of the 4-momentum transfer from the leptons to the hadrons, $\nu=E_\nu-E_{\mu^+}$;

$$\varepsilon=\frac{4E_\nu(E_\nu-\nu)-Q^2}{4E_\nu(E_\nu-\nu)+Q^2+2\nu^2}$$

is the polarisation parameter of the virtual intermediate boson; R is the ratio $\dfrac{d\sigma^L}{dt}\Big/\dfrac{d\sigma^T}{dt}$, where σ^L and σ^T are respectively the longitudinal and transverse ρ cross sections. Under the CVC hypothesis, R vanishes at $Q^2=0$; this is observed in photoproduction [10, 15]. In electro- and muoproduction, the Q^2 dependence of diffractive ρ^0 production up to $Q^2\sim10$ GeV^2 is well described by the VMD model with

$R=0$ [13, 16]; the value of R extracted from the ε dependence of the cross section is also compatible with 0 for Q^2 between 0.5 and 2 GeV^2 [16]. However, studies of the angular distributions of the ρ^0 decay products show that a large fraction of the ρ's are longitudinally polarized. Assuming s-channel helicity conservation (SCHC), and parametrizing R in the form $\xi^2 Q^2/m_\rho^2$, one finds $\xi^2 \sim 0.4$ at low Q^2 [27] and $R \sim 1$ at higher Q^2 [12]. Therefore, we compare our data to the model predictions for

(i) $R=0$, (5)

(ii) $R=0.4\,Q^2/m_\rho^2$, $R \leqq 1$. (6)

The ρ^- Ne elastic cross section is given by

$$\frac{d\sigma(\rho^- \mathrm{Ne} \to \rho^- \mathrm{Ne})}{dt} = \frac{A^2}{16\pi}\,\sigma_{\mathrm{tot}}^2(\rho^- N)\, e^{-b|t|}\, F_{\mathrm{abs}}, \quad (7)$$

where $A=20$ is the neon atomic number and $\sigma_{\mathrm{tot}}(\rho^- N)$ is the total ρ^--nucleon cross section at $E_\rho = \nu$ in the laboratory system. We take

$$\sigma(\rho^- N) = \sigma(\pi^- N), \quad (8)$$

which is supported by the experimental results on ρ^0 photoproduction on nuclei [28]. The slope parameter b is proportional to the transverse dimensions of the nucleus:

$$b = \alpha A^{2/3}. \quad (9)$$

The value of α, as extracted from data on coherent ρ^0 production on nuclei [29], is

$$\alpha = (10.8 \pm 0.4)\ \mathrm{GeV}^{-2}; \quad (10)$$

this value agrees with the one proposed by Rein and Sehgal [30] for the case of coherent single pion production, and used in [2]:

$$b = 1/3\,R_N^2,\ R_N = 1.12\,A^{1/3}\ \mathrm{fm}, \quad (11)$$

where R_N is the radius of the nucleus.

The factor F_{abs} in (7) accounts for the reinteraction of the ρ meson or of its decay products inside the nucleus. Experimental data on coherent ρ^0 production [31] give

$$F_{\mathrm{abs}} = 0.47 \pm 0.03. \quad (12)$$

The value of F_{abs}, when evaluated by simply treating the nucleus as a homogeneous sphere as proposed by Rein and Sehgal and used in [2], is 0.45, averaged over the SPS energy spectrum.

4 Comparison with the data

In order to evaluate the total cross section for ρ^- coherent production, several corrections have to be applied to the observed signal:

1. The coherent production of ρ mesons with $|t|$-values above 0.1 GeV^2 is evaluated to be $(15 \pm 3)\%$ using a Monte Carlo simulation based on (4) to (12), taking into account the experimental resolution. The error accounts for uncertainties on the simulation of measurement errors. It should be noted that the coherent signal increases from (33 ± 7) events for $|t| < 0.1$ GeV^2 to (38 ± 11) events for $|t| < 0.2$ GeV^2, while the Monte Carlo predicts 4 events for $|t|$ between 0.1 and 0.2 GeV^2.

2. Another major correction has to account for the coherent events in which one or two gammas from the π^0 decay escape detection in the bubble chamber. The gamma detection efficiency is evaluated from the gamma multiplicity distribution to be $(77 \pm 4)\%$ for 2-prong events, corresponding to a π^0 detection efficiency of $(59 \pm 6)\%$; in this rescanned sample, no evidence was found for a dependence of the detection efficiency with the π^0 momentum. The loss of γ's is incorporated in the Monte Carlo simulation according to the experimental conditions, the $|t|$-distributions for events with 1 or 2 detected gammas being different. The expected number of coherent events with only 1 detected gamma is (13 ± 5) for $|t| < 0.2$ GeV^2. This is to be compared to an observed coherent signal of (16 ± 10) events, including (3 ± 3) events attributed to single pion coherent production with emission of muon inner bremsstrahlung [2].

3. A third important correction evaluated by the Monte Carlo simulation is the effect of the p_{μ^+} cut. The loss of events with muon momentum < 5 GeV is estimated to be $(15 \pm 3)\%$ of the total number of coherent ρ^- events.

4. As in the case of coherent single pion production [2] the events with undefined charge due to an interaction of the π^- close to the vertex are discarded, and the remaining events are weighted according to the pion energy; the average weight is 1.085.

5. In addition, two minor corrections have to be made:
(i) after two different double scans for 2-prong events, the combined scanning efficiency for 2-prong events with gammas is $(97 \pm 3)\%$; (ii) (1 ± 1) apparent coherent $\mu^+ \pi^- \pi^0$ event is attributed to A_1 production with one of the π^0 mesons from the A_1 decay escaping detection in the bubble chamber.

The corrected number of events is thus (86 ± 23). The cross section for coherent ρ^- production in antineutrino charged current interactions is found to be $(95 \pm 25) \cdot 10^{-40}$ cm^2 per neon nucleus, averaged over

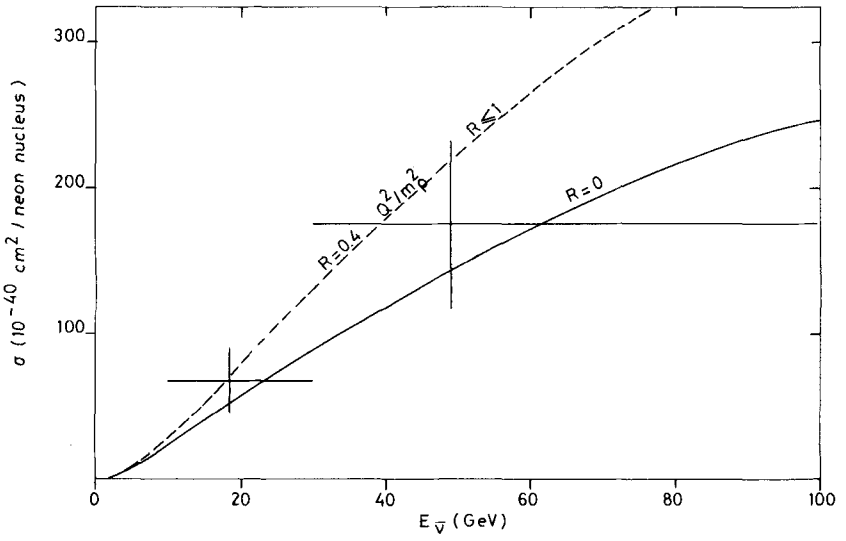

Fig. 6. Cross section for coherent ρ^- production by $\bar{\nu}_\mu$ charged current interactions on neon nuclei, as a function of the $\bar{\nu}$ energy $E_{\bar{\nu}}$; the curve is the prediction of the model (4) to (12) for two different assumptions on R: $R=0$ (solid curve) and $R=\xi^2 Q^2/m_\rho^2$, with $\xi^2=0.4$, $R \leqq 1$ (dashed curve)

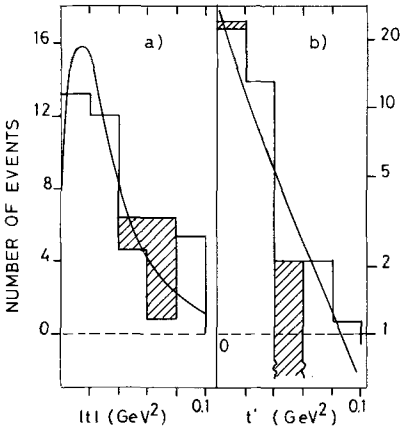

Fig. 7a, b. Distributions for **a** the square of the 4-momentum transfer t; **b** $t'=|t|-t_{\min}$ for the $\mu^+\pi^-\pi^0$ coherent events with $|t|<0.1$ GeV^2, weighted for the loss of events with undefined charge; the incoherent background, estimated from the events with stubs, is shown hatched. The curves, normalised to the coherent signal, are the predictions of the model (4) to (12), including the effects of experimental resolution

the SPS wide band beam energy spectrum. This number is determined using the total number of charged current $\bar{\nu}_\mu$ interactions in the present experiment (taking into account the 4% due to interactions on the H_2 in the liquid), and the known charged current antineutrino-nucleon cross section: $\sigma/E_{\bar{\nu}} = (0.35 \pm 0.02) \cdot 10^{-38}$ cm^2/GeV [32]. All the errors have been added in quadrature, including a 4% error due to the uncertainties in the flux shape.

The absolute value for the cross section of coherent ρ^- production in two energy bins ($E_{\bar{\nu}}<30$ GeV and $E_{\bar{\nu}}>30$ GeV) is shown in Fig. 6, and is compared with the Monte Carlo predictions based on (4) to (12). The data are in good agreement with the predictions of the VMD model, for both parametrizations of R. In our experimental conditions, (26 ± 4) events are predicted for $|t|<0.1$ GeV^2 in the case of (5) and (36 ± 6) of (6), whereas (33 ± 7) events are observed.

Differential distributions for the coherent signal are shown in Figs. 7 and 8 for the variables $|t|$, t', $E_{\bar{\nu}}$, ν, Q^2, W, x and y, where $t'=|t|-t_{\min}$, $t_{\min} \simeq \left(\frac{Q^2+m_\rho^2}{2\nu}\right)^2$ is the lower kinematic limit of $|t|$, $W=(2M_p\nu - Q^2 + M_p^2)^{1/2}$, $x=Q^2/2M_p\nu$ and $y=\nu/E_{\bar{\nu}}$ (M_p is the proton mass).

The 40 events with no stub at $|t|<0.10$ GeV^2 are displayed, and compared with the predictions of the Monte Carlo simulation. Among those events, (83 ± 9)% are estimated to be coherent; the background estimated by appropriately weighting the 4 incoherent events with stubs is subtracted from the distributions (the subtracted events are shown hatched). The mean values for the experimental distributions and for the Monte Carlo predictions are presented in Table 1. Agreement is observed between the data and the predictions of the model for all variables presented. This is true in particular for $\langle Q^2 \rangle$ *.

Figure 9 compares the ν, Q^2, x and y distributions for the coherent π^- and ρ^- events. Significant differ-

* Alternative forms for the Q^2-dependence, as suggested in [23], have also been tested. However, the agreement with the data is worse than in the case of the standard VMD model. The modified forms (ii) and (iii) in [23] predict significantly lower cross sections: for $R=0$, (10 ± 2) and (14 ± 2) events respectively are expected in our experimental conditions for $|t|<0.1$ GeV^2, whereas (33 ± 7) are observed (the predicted numbers of events should be multiplied by a factor ~ 1.4 for the case of the parametrization (6) of R). In the case of the modified form (i), which has a power $1/Q^2$ less than the VMD form, the predicted numbers of events are (19 ± 3) and (25 ± 4) respectively for the two parametrizations of R, but the mean ν and Q^2-values are significantly higher than the observed ones

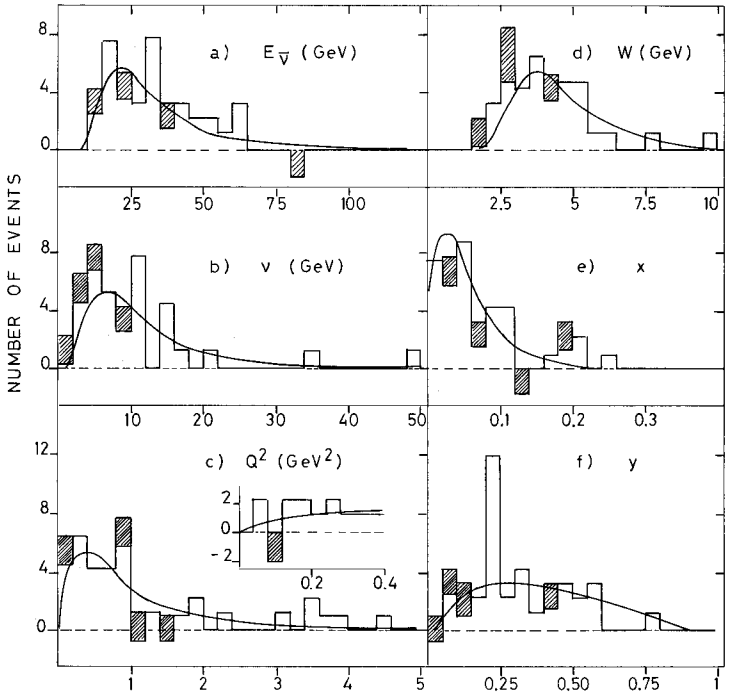

Fig. 8a–f. Distribution for **a** $E_{\bar{\nu}}$; **b** $\nu = E_{\bar{\nu}} - E_{\mu^+}$; **c** Q^2; **d** $W = (2M_p \nu - Q^2 + M_p^2)^{1/2}$; **e** $x = Q^2/2M_p \nu$; **f** $y = \nu/E_{\bar{\nu}}$ for the $(\mu^+ \pi^- \pi^0)$ coherent events with $|t| < 0.1$ GeV^2, weighted for the loss of events with undefined charge; the incoherent background, estimated from the events with stubs, is shown hatched. The curves, normalised to the coherent signal, are the predictions of the model (4) to (12), including the effects of experimental resolution, with the parameter R in (4) set to zero; the curves for $R = 0.4Q^2/m_\rho^2$, $R \leqq 1$ are almost indistinguishable from the curves shown

ences arise in the distributions of ν, Q^2 and y. In particular, the sharp peaking of the Q^2-distribution at low Q^2-values for the π^- events disappears in the case of the ρ^- events; this is because the conservation of the vector current (CVC) requires the Q^2 distribution to vanish at $Q^2 = 0$ in the case of diffractive vector meson production, whereas the non-conservation of the axial-vector current (PCAC) allows abundant π^- production at zero Q^2 via the coupling of the π^- meson to the longitudinal A_1. On the other hand, the x-distributions of the π^- and ρ^- events are similar, and essentially restricted to x-values < 0.2. This is kinematically linked to the small $|t|$-values of the coherent events; more generally, it is a necessary consequence of the fact that long distance hadronic fluctuations have to develop from the virtual W boson in order for it to interact coherently with the nucleus.

Table 1. Mean values of kinematical variables for the coherent $(\mu^+ \pi^- \pi^0)$ events with $p_{\mu^+} > 5$ GeV and $|t| < 0.1$ GeV^2, after background subtraction, compared to the predictions of the model (4) to (12), including the effects of experimental resolution; errors of the order of a few % arise on the model predictions for several variables because of the uncertainty in the flux shape. Two different contributions of longitudinal ρ production (R) are tested

		Data	Model	
			$R=0$	$R=0.4Q^2/m_\rho^2$ $R \leqq 1$
$E_{\bar{\nu}}$	(GeV)	30.6 ±3.9	37.9	39.5
P_μ	(GeV)	19.7 ±3.6	23.2	24.5
ν	(GeV)	10.9 ±1.9	14.6	14.9
p_{π^-}	(GeV)	6.0 ±1.4	7.5	7.7
p_{π^0}	(GeV)	5.0 ±1.0	7.2	7.3
Q^2	(GeV^2)	1.26 ±0.24	1.27	1.40
W	(GeV)	4.21 ±0.34	4.82	4.88
x		0.071 ±0.014	0.052	0.057
y		0.333 ±0.038	0.402	0.394
ε		0.891 ±0.025	0.827	0.837

The total and differential cross sections presented so far tell little about the value of R. In principle, the ρ decay angular distributions allow one to determine completely the ρ spin density matrix [24, 33]. In our experiment, the variable θ can reliably be measured, θ being the angle between the directions of the nucleus and the π^- in the ρ rest frame. The $\cos\theta$ distribution allows a measurement of one matrix element:

$$W(\cos\theta) \sim [1 - r_{00}^{04} + (3r_{00}^{04} - 1)\cos^2\theta]. \tag{13}$$

Assuming SCHC, – which is expected to hold for diffractive scattering, and in particular for coherent processes [19], – r_{00}^{04} is related to the helicity-zero ρ production and hence to the value of R:

$$R = \frac{\sigma^L}{\sigma^T} = \frac{1}{\varepsilon} \frac{r_{00}^{04}}{1 - r_{00}^{04}}. \tag{14}$$

Purely transverse ρ production ($r_{00}^{04} = 0$) would thus be characterized by a $\sin^2\theta$ distribution, and purely longitudinal ρ production ($r_{00}^{04} = 1$) by a $\cos^2\theta$ distribution. The value of r_{00}^{04} extracted from the $\cos\theta$ distribution presented in Fig. 10 is (0.41 ± 0.19); the para-

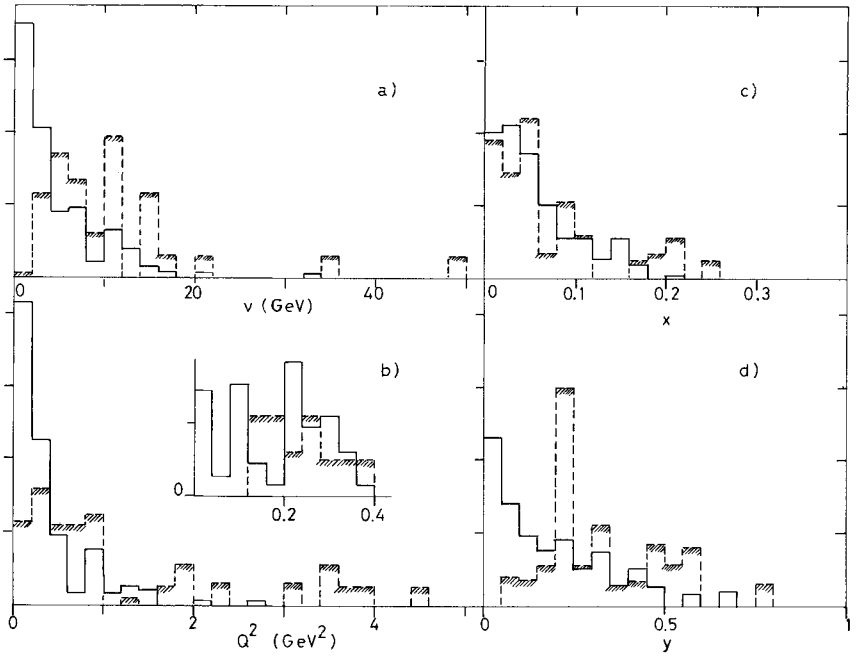

Fig. 9a–d. Distributions for **a** ν; **b** Q^2; **c** x; **d** y for the $\mu^+\pi^-\pi^0$ coherent events (shaded histograms) and for the $\mu^+\pi^-$ coherent events (solid histograms), normalised to each other

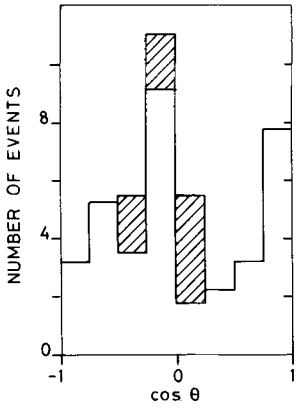

Fig. 10. Distribution of $\cos\theta$, the angle between the nucleus and the π^- directions in the ρ rest frame, for the $\pi^+\pi^-\pi^0$ coherent events with $|t|<0.1$ GeV^2, weighted for the loss of events with undefined charge; the incoherent background, estimated from the events with stubs, is shown hatched

metrization of R according to (6) predicts $\langle r_{00}^{04}\rangle = 0.32$. Our measured value agrees well with values obtained from exclusive ρ^0 meson electroproduction for similar Q^2-values [11, 12, 27], although [14] gives smaller values in muoproduction. Our result thus suggests a sizeable production of longitudinal ρ mesons.

5 Conclusions

In conclusion, using BEBC exposed to the CERN SPS $\bar{\nu}_\mu$ wide band beam, we have pursued the study of the exclusive channels contributing to the coherent charged current antineutrino-neon interactions by the analysis of the coherent production of ρ^- mesons. The corresponding cross section is measured to be $(95\pm25)\cdot10^{-40}$ cm^2 per neon nucleus, averaged over the beam energy spectrum. The distributions of kinematical variables and the absolute value of the cross section are in agreement with theoretical predictions based on the CVC hypothesis and the VMD model; the decay angular distribution suggests a sizeable production of longitudinal ρ mesons.

Acknowledgments. One of us (PM) acknowledges useful correspondance and discussions with A. Bartl, H. Fraas, W. Majerotto and L.M. Sehgal. We are pleased to acknowledge the excellent work of the SPS, BEBC and EMI crews; we also thank our scanning and measuring teams for their careful work.

References

1. P. Marage et al.: Phys. Lett. **140B**, 137 (1984)
2. P. Marage et al.: Z. Phys. C – Particles and Fields **31**, 191 (1986)
3. WA 59 Collaboration: Study of Coherent Production of ρ^- Mesons by Charged Current Antineutrino Interactions in BEBC. Paper submitted to the XII Conference on Neutrino Physics and Astrophysics, Sendai, 1986
4. D. Picard: Production Cohérente des Mésons Vecteurs dans l'Expérience Wide-Band du PS, LAL-79/38, unpubl.
5. A. Bouchakour: Thesis, Strasbourg (1980), unpubl.
6. H.C. Ballagh et al.: Observation of Coherent ρ Production in Neutrino-Neon Interactions. Paper submitted to the XII Conference on Neutrino Physics and Astrophysics, Sendai, 1986

7. J. Bell et al.: Phys. Rev. Lett. **40**, 1226 (1978)
8. D.R.O. Morrison: Proceedings of the 1978 International Meeting on Frontier of Physics, K.K. Phua, C.K. Chew and Y.K. Lim (eds.) Singapore National Academy of Science, 205 (1978)
9. V.V. Ammosov et al.: Sov. J. Nucl. Phys. **42**, 236 (1985)
10. T.H. Bauer et al.: Rev. Mod. Phys. **50**, 261 (1978), and references therein
11. C. Del Papa et al.: Phys. Rev. **D19**, 1303 (1979)
12. D.G. Cassel et al.: Phys. Rev. **D24**, 2787 (1981)
13. I. Cohen et al.: Phys. Rev. **D25**, 634 (1982)
14. W.D. Shambroom et al.: Phys. Rev. **D26**, 1 (1982)
15. D. Aston et al.: Nucl. Phys. **B209**, 56 (1982)
16. J.J. Aubert et al.: Phys. Lett. **161B**, 203 (1985)
17. P. Söding: Phys. Lett. **19**, 702 (1966)
18. M. Ross, L. Stodolsky: Phys. Rev. **149**, 1172 (1966)
19. L. Stodolsky: Coherence in High Energy Reaction, in: Proc. Intern. School of Elem. Part. Phys. p. 259, (Herceg-Novi, 1968), New-York: Gordon and Breach 1970. See also in: Methods in Subnuclear Physics, vol. V, p. 151, New York: Gordon and Breach 1977
20. The form of the cross section has been given by several authors, among others in [21–25]. However, discrepancies appear between them concerning numerical factors. In [22, 25], a factor 1/2 is missing with respect to (4) (in addition, (20) of [22] should be read with a factor $1/2\pi^3$ instead of $1/(2\pi)^3$ for internal consistency within that paper). On the other hand, a factor of 2 is missing in (2) of [23]; this is probably due to a missing normalisation factor $\sqrt{2}$ in the definition of the charged current-meson coupling constant f_V, which should read $f_V = \sqrt{2} m_V^2/\gamma_V$, with $\gamma_\rho^2/4\pi \sim 2.4$ (see p. 349). These differences probably explain part of the discrepancies noted by the authors of [23] and [25] in their discussion of the results of [7]
21. C.A. Piketty, L. Stodolsky: Nucl. Phys. **B15**, 571 (1970)
22. M.K. Gaillard, S.A. Jackson, D.V. Nanopoulos: Nucl. Phys. **B102**, 326 (1976); Nucl. Phys. **B112**, 545 (1976)
23. M.S. Chen, F.S. Henyey, G.L. Kane: Nucl. Phys. **B118**, 345 (1977)
24. A. Bartl, H. Fraas, W. Majerotto: Phys. Rev. **D16**, 2124 (1977)
25. M.K. Gaillard, C.A. Piketty: Phys. Lett. **68B**, 267 (1977)
26. See P. Callahan et al.: ρ Photoproduction from 45 to 225 GeV, Fermilab-Pub 84/36-E. However, the analysis of [10] favours value of $\gamma_\rho^2/4\pi$ around 2.1 (see discussion p. 387 and table XXXIII); the predicted cross sections should be scaled accordingly
27. P. Joos et al.: Nucl. Phys. **B113**, 53 (1976)
28. See [10], Table XXXIII, p. 387
29. This value is obtained from the t' dependence of the cross section for $690 < m_{\pi\pi} < 870$ MeV, combining data for $p_\gamma = 5.8$, 6.2 and 6.6 GeV, for C, Al and Cu, in H. Alvensleben et al.: Nucl. Phys. **B18**, 333 (1970); see also J.G. Asbury et al.: Phys. Rev. Lett. **19**, 865 (1967), H. Blechschmidt et al.: Nuovo Cimento **52A**, 1348 (1967)
30. D. Rein, L.M. Sehgal: Nucl. Phys. **B223**, 29 (1983); The parametrization of (11) is close to the results obtained from hadron-nucleus scattering – see A. Schiz et al.: Phys. Rev. **D21**, 3010 (1980)
31. Interpolation for neon of the data presented by H. Alvensleben et al. [29], Fig. 7 and p. 361, and by G. Mc Clellan et al.: Phys. Rev. **D4**, 2683 (1971), Fig. 6, p. 2690
32. M. Aderholz et al.: Phys. Lett. **173B**, 211 (1986)
33. K. Schilling, G. Wolf: Nucl. Phys. **B61**, 381 (1973)